Automatic image registration of multi-temporal KOMPSAT-2 images in agricultural areas

Youkyung Han, Junho Yeom, Yeji Kim and Yongil Kim*
Department of Civil and Environmental Engineering, Seoul National University, Seoul 151-742, REPUBLIC OF KOREA
***yik@snu.ac.kr**

Abstract

The objective of this study is to extract well-distributed matching points in agricultural areas having many similar patterns of farming intensity and homogeneous paddies. Mutual information (MI) which is one of the representative intensity-based similarity measures was used to estimate the initial translation difference between multi-temporal high-resolution images. Regular grids were then constructed over the entire images based on the initial translation and the center points of each grid were evaluated as the candidate points for precise matching.

Based on these points, corresponding points were determined as the final matching points using the MI method. Multi-temporal high-resolution satellite images from Korea Multi-purpose Satellite-2 (KOMPSAT-2), which was launched in 2006 and has 1 m spatial resolution, were used for the experiments. Using the proposed method, we were able to extract evenly distributed matching points over the entire image and we obtained acceptable registration accuracies for all sites.

Keywords: Agricultural areas, Automatic image registration, High-resolution multi-temporal data, KOMPSAT-2, Mutual information.

Introduction

The monitoring of crop conditions to predict crop yields is of critical economic importance in the world's competitive markets. To accomplish this monitoring, remote sensing has been applied to agricultural fields during the past several decades due to the periodic accessibility of remote sensing images. Multi-temporal satellite images are commonly used to determine seasonal changes in crop conditions and to predict the crop yields based on statistical correlations between the multiple-wavelength reflectance data obtained by the sensors and the actual crop conditions. To use remote sensing data for seasonal analysis, multi-temporal images should be precisely co-registered. For this reason, image registration is one of the fundamental preprocessing steps for seasonal crop analysis.

Image registration is the process of geometrically overlaying two or more images of the same scene[16]. Most image registration methods employ four main steps. In the first step, features, which are the objects that correspond to distinct and representative points, are extracted from each image. Next, each feature from one image is matched with the corresponding feature of the other image using a similarity measure. A transformation model is then constructed with the matching points using a linear or non-linear function. Finally, one of the images is registered to the other image. The matching points are typically extracted manually which requires considerable human resources, cost and time. Therefore, there has been considerable interest in the development of automatic image-to-image registration.

Most studies of automatic registration between high-resolution images have used feature-based methods for the extraction of matching points. Feature extraction methods or matching methodologies appropriate for image registration between high-resolution images have been proposed[5, 7, 14, 15]. For example, a scale-invariant feature transform (SIFT) method, which was introduced by Lowe[10] for extracting and matching features, is representative and appropriate for image registration between high-resolution images[6, 9, 15]. However, the SIFT method cannot consider the distribution of the extracted matching points and the matching-point pairs between images must be distributed evenly over the entire area of both images for the accurate registration of high-resolution images. Agricultural areas used for rice cultivation in particular contain many similar and homogeneous paddies, making it difficult to extract the matching points. Furthermore, seasonal changes in paddies preclude the measurement of the spectral similarity between images. Therefore, it is difficult to co-register between high-resolution images in agricultural areas using feature-based method.

An intensity-based method, which does not attempt to detect salient features in images, is suitable for the image registration of agricultural areas. Commonly used intensity-based methods include the cross-correlation (CC) and mutual information (MI) methods. The CC method uses the direct matching of image intensity and is sensitive to changes in intensity. Seasonal changes in paddy fields cause intensity changes and thus, the CC method is not appropriate. As an alternative to CC method, the MI method is typically used for multimodal registration applications, such as high-resolution optical and synthetic aperture radar (SAR) images used in remote sensing[2, 3, 12]. MI method is also appropriate for the registration of multi-temporal images that capture seasonal changes in paddy fields of agricultural areas.

The objective of this study is to extract well-distributed

matching points in agricultural areas that have many similar patterns of farming intensity and homogeneous paddies. The MI method was used to estimate the initial translation difference between multi-temporal high-resolution images. Regular grids were then constructed over the entire image and center points of each grid were evaluated as the candidate points for precise matching. Based on these points, corresponding points were determined as the final matching points using the MI method. Multi-temporal high-resolution satellite images obtained by the Korea Multi-purpose Satellite-2 (KOMPSAT-2), which was launched 2006 and has a 1 m spatial resolution for panchromatic images and 4 m spatial resolution for multispectral images, were used for the experiments.

Material and Methods

A flowchart of the proposed method for the automatic registration between multi-temporal KOMPSAT-2 images in agricultural areas is shown in figure 1. First, an MI-based similarity measure is used to estimate the initial translation in the x and y directions between the reference and target images. Pyramid images of each image are generated to reduce the computation time and estimate the global extreme through a simulated annealing optimization method. The reference image is then divided regularly over the entire image and central points arranged in each regular grid are selected as the center of the template to extract the evenly distributed matching points.

The corresponding center of the templates of the reference image is also selected based on the estimated initial translation between two images. The corresponding templates are used to find the local precise matching points when the calculated value of the MI is larger than a threshold that is predefined using a simplex optimization method. Outliers that are incorrectly located geometrically are eliminated from the matching-point set using an RANSAC algorithm and the affine transformation coefficient is estimated from remained matching points. Finally, the target image is transformed to the reference coordinate system using the affine transformation.

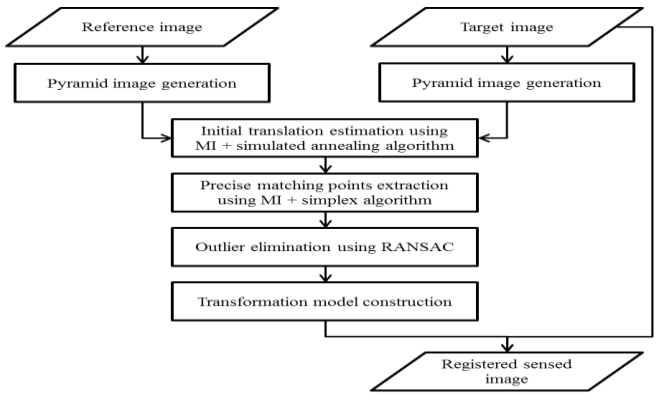

Figure 1: Flowchart of the proposed method

MI method: To estimate the x and y translations of the two images, this study uses the MI method which is a typical intensity-based similarity measurement. The MI method was first introduced for the geometric correction of images obtained from the multi-sensors of medical imaging systems[13]. The MI method matches two images by measuring their statistical correlation. The MI value of images A and B can be calculated using the following equation, in which a larger measured value corresponds to a greater similarity between two images.

$$\mathrm{MI(A,B)} = \mathrm{H(B)} - \mathrm{H(B|A)} = \mathrm{H(A)} + \mathrm{H(B)} - \mathrm{H(A,B)} \quad (1)$$

Here, H(A) and H(B)are the entropy of images A and B respectively and H(A,B) is the joint entropy of images A and B. These parameters can be calculated as follows:

$$\mathrm{H(A)} = -\sum_a p_A(a) \log_{p_A}(a) \quad (2)$$

$$\mathrm{H(B)} = -\sum_b p_B(b) \log_{p_B}(b) \quad (3)$$

$$\mathrm{H(A,B)} = -\sum_{a,b} p_{A,B}(a,b) \log_{p_{A,B}}(a,b) \quad (4)$$

where $\mathrm{p_A(a)}$ and $\mathrm{p_B(b)}$ are the probability distribution of images A and B respectively and $\mathrm{p_{A,B}(a,b)}$ is the joint probability density function of A and B. The joint probability density function can be calculated as follows:

$$p_{A,B}(a,b) = \frac{h(a,b)}{\sum_{a,b} h(a,b)} \quad (5)$$

$$p_A(a) = \sum_b p_{A,B}(a,b) \quad (6)$$

$$p_B(b) = \sum_a p_{A,B}(a,b) \quad (7)$$

Here, *h(a,b)* represents the joint histogram of two images *A* and *B*. The joint histogram is arranged in 2 dimensions, where the pixel value *a* for image *A* is one axis and the pixel value *b* for image *B* is the other axis.

Initial estimation of the translation using global MI: To estimate the translation at the sub-pixel level between reference and target images, this study proposes an integrated methodology using image pyramid and MI methods. When the MI value is calculated from the original image, it not only requires a great deal of calculation time but also has the risk of drawing out the local extreme due to the limit of the searching space. Therefore, for the coarsest image of the pyramid generated through the image pyramid method that incrementally reduces the spatial resolution of image, the initial translation value is estimated using an optimization technique that considers the MI value as its objective function.

Using this method to set the MI value as the objective function and to apply the optimization technique for the coarsest level of the pyramid image, the calculation cost

can be reduced and the global optimum value can be found, even when the positions of the initial two images are greatly different. Therefore, by using the simulated annealing algorithm known to be suitable for identifying the global optimum, the optimum value of the translation between two images on the uppermost pyramid is estimated[1].

Precise matching point extraction using local MI: After the estimated amount of translation is set as the initial value for the extraction of precise matching points for the construction of the transformation model, the points are arranged in regular grids on the reference image and points on the corresponding grids are also constructed on the target image which is shifted based on the estimated translation in the x and y directions. Matching points are then extracted from corresponding points using an optimization method that considers the MI value as its objective function and a value that is higher than the predefined threshold. The simplex optimization method, which has better calculation efficiency than the simulated annealing method and does not require the establishment of the searching space, is used for the extraction of matching points[8, 11]. The outlier elimination process is performed using the RANSAC algorithm[4] and the coefficients of the affine transformation are estimated from the remaining matching points.

Results and Discussion

Study site and data: The study site is an agricultural area in Daejeon, South Korea. Four scenes from three multi-temporal KOMPSAT-2 images were used for the experiment. KOMPSAT-2 was launched on 28 July 2006 and the primary missions include the observation of natural resources and atmospheric conditions and the creation of digital and thematic maps. The KOMPSAT-2 sensor produces a panchromatic image with 1m spatial resolution and four multispectral images with 4m spatial resolution. The radiometric resolution of the sensor is 10 bits. The specifications of the KOMPSAT-2 images are shown in table 1.

Two study sites having a combination of three KOMPSAT-2 panchromatic images were selected. The reference image of site 1 was acquired on May 6th 2008 and has an off-nadir angle of 14.03°. The target image of site 1 and reference image of site 2 were acquired on September 13th 2008; these images have an off-nadir angle of 19.55°. The target image of site 2 was acquired on May 10th 2007 and has an off-nadir angle of 28.40°. Histogram equalization was applied to enhance the contrast of all images which were then transformed to 8-bit radiometric resolution as a preprocessing step to aid in the extraction of the matching points. The preprocessed images of the study sites are shown in figure 2.

Table 1
Sensor specification of KOMPSAT-2

Sensor	KOMPSAT-2
Spatial resolution	Panchromatic : 1m Multispectral : 4m
Band wavelength	Panchromatic: 500-900nm Multispectral: Band 1 (Blue): 450nm - 520nm Band 2 (Green): 520nm - 600nm Band 3 (Red): 630nm - 690nm Band 4 (NIR): 760nm - 900nm
Radiometric resolution	10bits
Swath width	15km
Altitude	685.13km

Experiment: The initial estimation of the translation in the x and y directions using global MI resulted in a shift of 3.08 pixels in the x-direction and 6.14 pixels in y-direction for site 1 and a shift of -5.77 pixels in the x-direction and 18.63 pixels in the y-direction for site 2. Evenly distributed features were extracted by constructing regular grids over the entire image and the templates were produced based on each feature. To extract a corresponding template from the target image, templates of the same size were generated after relocating the central points of the target image relative to the shift due to the initial translation estimation in the x and y directions. In this study, the features were extracted at a 25×25 pixel resolution and the templates were generated at a size of 128×128 pixels.

(a) site 1 **(b) site 2**

Figure 2: Study sites after the preprocessing step

As a result, 473 matching pairs were extracted in site 1 and 129 matching pairs were extracted in site 2 (Figure 3). RANSAC was then applied to the extracted matching pairs to remove the outliers for the affine transformation model estimation and 255 and 37 pairs were extracted individually for sites 1 and 2 respectively (Figure 4). Table 2 indicates the number of matching pairs extracted by the MI method only and the MI method after the removal of outliers using RANSAC.

A greater number of matching points was extracted in site 1 than in site 2. This difference may have been due to the spectral difference between the reference and target images in site 2, as the majority of the area of site 2 was occupied by paddy fields and both seasonal and temporal differences were present. Therefore, some of the matching pairs could not be extracted from the paddy fields. However, the number of extracted matching points in site 2 was sufficient to co-register between two images. Site 1, on the other hand, contained not only paddy fields but also other areas such as roads and bare soil. Therefore, relatively high number of matching pairs in site 1 could be extracted compared to the number of matching pairs in site 2, although seasonal differences were observed between reference and target images individually taken in May and September.

Using the extracted matching pairs, an affined model was estimated and the target image was transformed to the coordinate system of the reference image. Figure 5 shows the result of mosaic image generation after standardizing the coordinate system between the two images. In figure 5, the reference image is represented in red blocks and the geometrically corrected target image is represented in gray blocks. By comparing the red and gray blocks in figure 5, we can visually confirm that the geometric correction between the two images was processed properly. To perform an accuracy assessment, 20 well-distributed checkpoints for each site were manually extracted to estimate the bias, standard deviation, root mean square error (RMSE) and circular error of 90% (CE90) (Table 3).

The results showed small biases for all sites, indicating that there is no systematic error and affine transformation can explain the geometric properties between two images. In the accuracy test, site 1 showed an RMSE of 2.39m of and CE90 of 3.61m, whereas site 2 shows an RMSE of 1.64m and CE90 of 2.51m. Site 2 showed better overall accuracy with respect to the geometric correction relative to site 1, although fewer matching points were extracted for site 2 than for site 1. This difference may have occurred because site 2 was mainly composed of many paddy fields which have relatively flat regions. A flat region can lead to less local distortion caused by relief displacement, presenting better registration accuracy. The result for both of the sites, however, presented less than 2.5m RMSE and we could confirm the reliable accuracy of the geometric correction results for both sites.

Table 2
Number of extracted matching points

Site	Number of extracted matching points (pairs)	
	GMI + LMI	After RANSAC
1	473	255
2	129	37

Table 3
Registration accuracy

Site	Bias (m)		Std. (m)		RMSE(m)	CE90 (m)
	x	y	x	y		
1	0.40	0.16	1.98	1.28	2.39	3.61
2	1.00	0.13	0.90	1.01	1.64	2.51

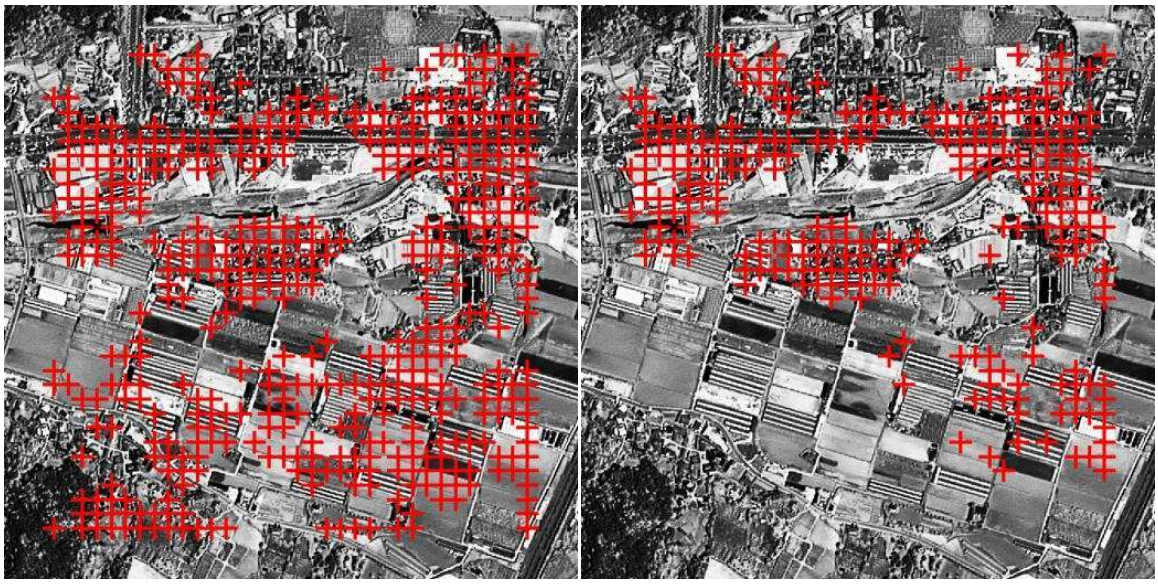

Figure 3: Extracted matching points obtained by the proposed method: (a) site 1 (b) site 2

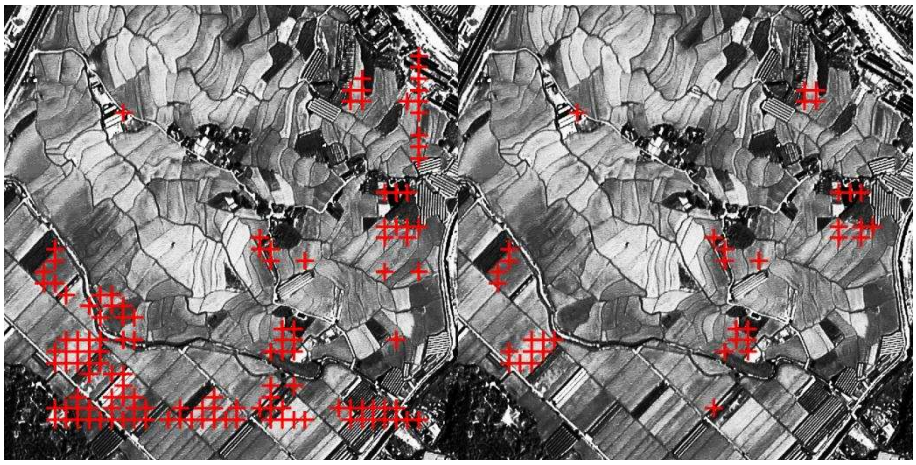

Figure 4: Extracted matching points after RANSAC: (a) site 1 (b) site 2

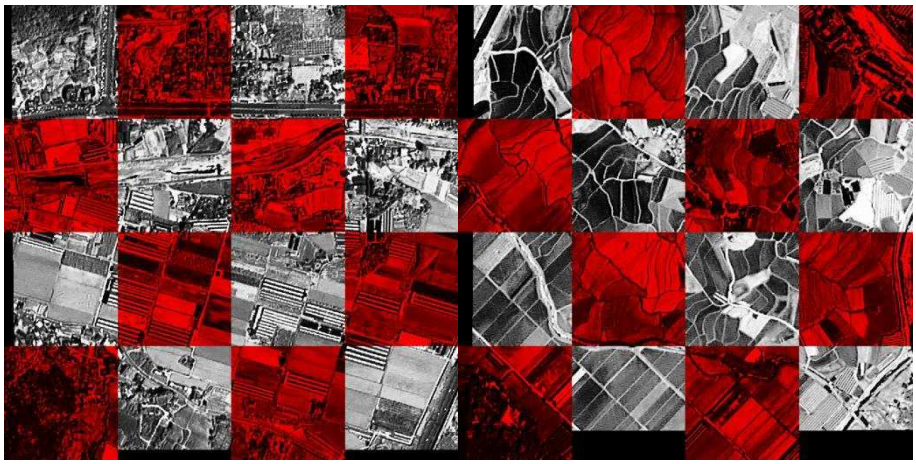

Figure 5: Mosaic image generation by the proposed method: (a) site 1 (b) site 2

Conclusion

We have proposed an automatic image registration method for agricultural areas having similar patterns of farming intensity and homogeneous paddies. Multi-temporal KOMSAT-2 images were used for the experiments. The MI method was used for estimating the initial translation difference between images and for extracting the matching points. The results demonstrated that the method can extract a suitable number of matching points even though the agricultural areas have many similar patterns and few salient points. The registration results obtained using the proposed method were highly accurate, with an RMSE of approximately 2.5 m in all study sites. The distribution of matching points, however, must be considered to further increase the level of accuracy.

Acknowledgement

This work was supported by the National Research Foundation of Korea (NRF) grant funded by the Korea government (MEST) (No. 2012R1A2A2A01045157).

References

1. Ali M., Torn A. and Viitanen S., A direct search variant of the simulated annealing algorithm for optimization involving continuous variables, *Computer & Operations Research*, **29(1)**, 87-102 **(2002)**

2. Chen H., Arora M. and Varshney P., Mutual information-based registration for remote sensing data, *International Journal of Remote Sensing*, **24(18)**, 3701-3706 **(2003)**

3. Cole-Rhodes A., Johnson K., LeMoigne J. and Zavorin I., Multiresolution registration of remote sensing imagery by optimization of mutual information using a stochastic gradient, *IEEE Transactions on Image Processing*, **12(12)**, 1495-1511 **(2003)**

4. Fischler M. and Bolles R., Random sample consensus: A paradigm for model fitting with applications to image analysis and automated cartography, *Communications of the ACM*, **24(6)**, 381–395 **(1981)**

5. Gianinetto M. and Scaioni M., Automated geometric correction of high-resolution pushbroom satellite data, *Photogrammetric Engineering and Remote Sensing*, **74(1)**, 107-116 **(2008)**

6. Han Y., Byun Y., Choi J., Han D. and Kim Y., Automatic registration of high-resolution images using local properties of

features, *Photogrammtric Engineering and Remote Sensing*, **78(3)**, 211-221 **(2012)**

7. Hong G. and Zhang Y., Wavelet-based image registration technique for high-resolution remote sensing images, *Computers & Geosciences*, **34(12)**, 1708-1720 **(2008)**

8. Lagarias J., Reeds J., Wright M. and Wright P., Convergence properties of the Nelder-Mead simplex method in low dimensions, *SIAM Journal of Optimization*, **9(1)**, 112-147 **(1998)**

9. Li Q., Wang G., Liu J. and Chen S., Robust scale-invariant feature matching for remote sensing image registration, *IEEE Geoscience and Remote Sensing Letters*, **6(2)**, 287-291 **(2009)**

10. Lowe D., Distinctive image features from scale-invariant keypoints, *International Journal of Computer Vision*, **60(2)**, 91-110 **(2004)**

11. Nelder J. and Mead R., A simplex method for function minimization, *The Computer Journal*, **7(4)**, 308-313 **(1965)**

12. Shu L., Tan T., Tang M. and Pan C., A novel registration method for SAR and SPOT images, International Conference on Image Processing, **2**, 213-216 **(2005)**

13. Viola P. and Wells W., Alignment by maximization of mutual information, *International Journal of Computer Vision*, **24(2)**, 137-154 **(1997)**

14. Xiong Z. and Zhang Y., A novel interest-point-matching algorithm for high-resolution satellite images, *IEEE Transactions on Geoscience and Remote Sensing*, **47(12)**, 4189-4200 **(2009)**

15. Yu L., Zhang D. and Holden E., A fast and fully automatic registration approach based on point features for multi-source remote-sensing images, *Computers & Geosciences*, **34(7)**, 838-848 **(2008)**

16. Zitova B. and Flusser J., Image registration methods: A survey, *Image and Vision Computing*, **21(11)**, 977-1000 **(2003).**

(Received 15th May 2013, accepted 21st September 2013)